Bioorganic & Medicinal Chemistry Letters 18 (2008) 4569–4572

Contents lists available at ScienceDirect

Bioorganic & Medicinal Chemistry Letters

journal homepage: www.elsevier.com/locate/bmcl

Discovery of piperidine carboxamide TRPV1 antagonists

Wing S. Cheung, Raul R. Calvo, Brett A. Tounge, Sui-Po Zhang, Dennis R. Stone, Michael R. Brandt, Tasha Hutchinson, Christopher M. Flores, Mark R. Player *

Johnson & Johnson Pharmaceutical Research and Development, Welsh and McKean Roads, Spring House, PA 19477, USA

ARTICLE INFO

Article history:
Received 27 May 2008
Revised 8 July 2008
Accepted 10 July 2008
Available online 15 July 2008

Keywords:
TRPV1
VR1
Capsaicin

ABSTRACT

A series of piperidine carboxamides were developed as potent antagonists of the transient receptor potential vanilloid-1 (TRPV1), an emerging target for the treatment of pain. A focused library of polar head groups led to the identification of a benzoxazinone amide that afforded good potency in cell-based assays. Synthesis and a QSAR model will be presented.

A variety of potentially damaging chemical, thermal, and mechanical stimuli can elicit signals from peripheral nerve endings, ultimately leading to the perception of pain. These nerve endings are small diameter sensory neurons known as nociceptors. The transient receptor potential vanilloid 1 (TRPV1) is found on nociceptive primary afferents of C- and Aδ-fibers, and is considered to be a key polymodal integrator of noxious sensations.[1] It is activated by heat, low pH, and endogenous lipidic mediators, such as anandamide, as well as by pungent natural products such as capsaicin and resiniferatoxin.

TRPV1 agonists cause calcium influx, depolarization, and an initial sensation of pain. Activation over time causes physiologic changes to the nociceptor resulting in desensitization and a subsequent period of analgesia. Thus, local exposure to capsaicin has been shown to provide pain relief in humans, though the irritancy of TRPV1 agonists to date limits their application to primarily topical indications. Collectively, these findings have inspired intense pharmaceutical interest in exploring the potential utility of orally bioavailable TRPV1 antagonists as therapies for acute and chronic pain. Presently, GlaxoSmithKline (SB705498), Neurogen/Merck (NGD-8243/MK-2295), and Lilly/Glenmark (GRC-6211) are investigating TRPV1 antagonists in phase II trials for acute pain.[2] Herein, we describe our findings on a carboxamide series of TRPV1 antagonists.

Our initial work identified a class of piperidine carboxamides such as **1** (Table 1), which behaved as weak antagonists of the TRPV1 receptor. Similar to other prototypical piperazine carboxamides,[3] the structure could be divided into three components: polar head, linker, and hydrophobic tail (Table 1). Keeping the linker fixed, we elected to explore the SAR of the polar head and hydrophobic tail regions.

The various piperidine carboxamides were synthesized as shown in Scheme 1.[4] The piperidine acid (Method A) or ester precursor (Method B) was subjected to Pd-mediated arylation. Subsequent amide formation by either EDC (Method C) or acid chloride-mediated coupling (Method D) afforded the desired compounds, which were purified by silica gel chromatography.

We initially explored the addition of a number of different heterocycles in the polar head group region. The isomeric 2,3-dihydro-1*H*-indoles **2**–**4** (Table 1) showed the sensitivity to changes in this part of the polar region. Compound **3** exhibited activity but **2** and **4** were devoid of potency. Indole **5** showed increased potency but isomer **6** was fourfold less potent. Indole isomer **7** was inactive, illustrating the importance of examining amide substitution position with each heterocycle explored. From this exercise, 4*H*-benzo[1,4]oxazin-3-one **8** was found to be a moderately potent antagonist in a functional assay with an IC_{50} of 180 nM and a K_i of 65 nM in a hTRPV1 binding assay.[5] Next, various substituents were placed on the phenyl ring in the nonpolar tail region of **9** to examine the effect on functional potency (Table 2). In order to better understand the nature of the substituent effects, a QSAR model was constructed.

Compounds **8**–**29** were used to construct the QSAR model. The compounds were first subjected to Ligprep to generate an initial set of 3D coordinates.[6] Next, a set of low energy conformations was generated for each ligand using the Monte Carlo Multiple Minimum (MCMM) method in MacroModel (OPLS-2005, water, $\varepsilon = 1$, 40 kJ/mol energy window, 1000 steps).[7] Using these conformations as input, a Phase common pharmacophore was built for the top 4

* Corresponding author. Tel.: +1 610 458 6980; fax: +1 610 458 8258.
E-mail address: mplayer@its.jnj.com (M.R. Player).

0960-894X/$ - see front matter © 2008 Elsevier Ltd. All rights reserved.
doi:10.1016/j.bmcl.2008.07.035

Table 1
Human TRPV1 functional potencies of polar head substituents

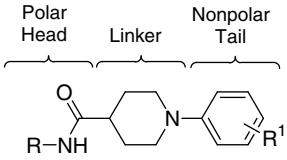

Compound	R	R^1	Functional potency IC_{50} (nM)
1	Quinolin-3-yl	3-CF_3	600
2	1-Acetyl-2,3-dihydroindol-7-yl	3-CF_3	5610
3	1-Acetyl-2,3-dihydroindol-6-yl	3-CF_3	800
4	1-Acetyl-2,3-dihydroindol-5-yl	3-CF_3	>9000
5	Indol-4-yl	3-CF_3	230
6	Indol-5-yl	3-CF_3	1070
7	Indol-6-yl	3-CF_3	>9000
8	3-Oxo-3,4-dihydrobenzo[1,4]oxazin-6-yl	3-CF_3	180

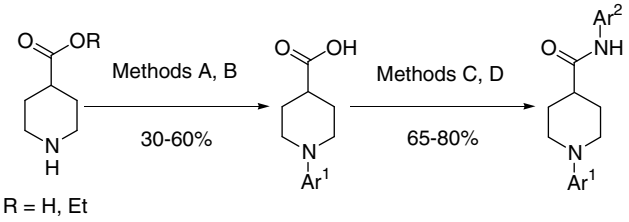

Scheme 1. Reagents and conditions: Method A (R = H): $Pd(OAc)_2$, 2-(tBu)$_2$P-biphenyl, NaO^{t}Bu, Ar^1X, THF, 65 °C; Method B (R = Et): (a) $Pd(P(tBu)_3)_2$, K_3PO_4, Ar^1X, DME, 100 °C; (b) MeOH, LiOH, 80 °C, 3 h; Method C: EDC, HOBt, Et_3N, DMF, Ar^2NH_2, rt; Method D: oxalyl chloride, CH_2Cl_2, Et_3N, Ar^2NH_2, 0 to 25 °C.

Table 2
Human TRPV1 binding affinities and functional potencies of nonpolar tail substituents

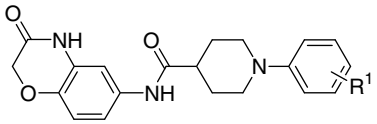

Compound	R^1	Binding affinity K_i (nM)	Functional potency IC_{50} (nM)
9	H	—	1810
10	3-Fluoro	84	520
11	3-Chloro	97	190
12	3-Bromo	—	330
13	3-Methoxy	—	1420
14	3-Methyl	225	490
15	2-Fluoro	1470	670
16	2-Chloro	93	220
17	2-Bromo	71	160
18	2-Trifluoromethyl	68	380
19	2-Nethyl	61	150
20	2-Ethyl	125	150
21	2-Isopropyl	78	180
22	2-Bromo-3-fluoro	81	130
23	2-Methyl-3-chloro	100	100
24	2,3-Dimethyl	28	60
25	4-*t*-Butyl	142	90
26	3,4-Difluoro	56	850
27	3,4-Dimethyl	314	380
28	3,5-Difluoro	137	370
29	3,4,5-Trifluoro	49	59

compounds based on functional activity (**23**–**25**, **29**).[8] This model was then used to align all the molecules in the QSAR training set (Fig. 1). Finally, for each aligned pose several descriptors were

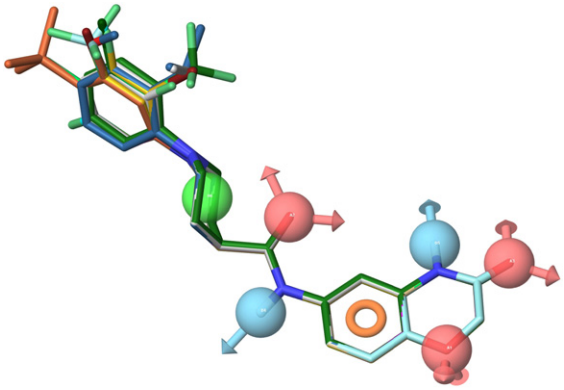

Figure 1. Overlay of the twenty-two model compounds as obtained from the Phase pharmacophore model. Red → hydrogen bond acceptor, Blue → hydrogen bond donor, Orange → aromatic, and Green → hydrophobic.

calculated. These included $c\log P$ and the set of descriptors from QuickProp.[9,10]

To assess the best descriptors to use in terms of fitting the TRPV1 functional activity data ($pIC_{50} = -1.0 * \log$ (Functional Activity IC_{50})), a stepwise multiple linear regression run was performed using the JMP statistics package.[11] One compound (**29**) in the training set could not be fit to the same trends as the remaining 21 ligands, so it was removed from the final model. The final QSAR model obtained was limited to a 3-parameter fit:

$$pIC_{50} = 29.4007 + 0.5893 * c\log P - 0.2214 * \mathrm{FISA}, \quad (1)$$

where FISA is the hydrophilic solvent accessible surface area as calculated in QuickProp. The model yielded an $r^2 = 0.71$ and a root mean squared error (RMSE) = 0.22 (Fig. 2).

The QSAR model contains two terms that capture the hydrophobic/hydrophilic nature of these TRPV1 compounds. Compounds with a large $c\log P$ values (i.e., more hydrophobic) exhibited higher functional potency. Since, in the ligand training set, we have focused on changes in the tail region (the generally more hydrophilic head is fixed), this means that the tail region in particular favors hydrophobic moieties. While the 2D $c\log P$ descriptor captures a large part of the variation seen in the TRPV1 functional activity, the 3D conformation-dependent FISA term improves the fit markedly. We see in this term a penalty for any solvent-exposed hydrophilic surface area. For example, this can be seen in the methoxy-substituted phenyl ring of **13**.

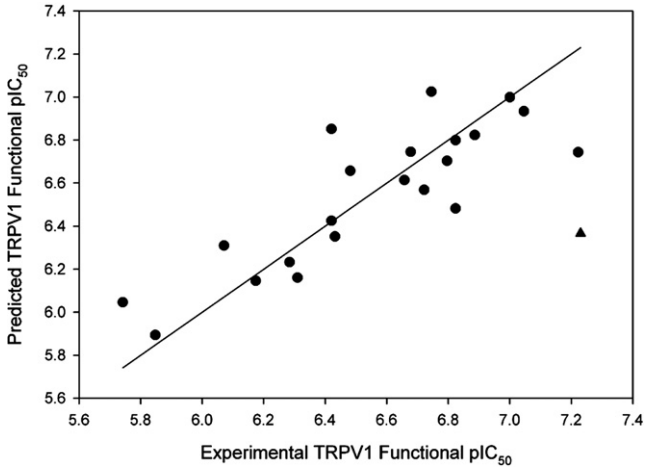

Figure 2. Final QSAR model for the functional activity of compounds **7**–**26** ($r^2 = 0.71$, RMSE = 0.22). Compound **29** could not be fit (red triangle in above plot).

Table 3
Stability in human and rat liver microsomes

Compound	HLM Stability $t_{1/2}$ (min)	RLM Stability $t_{1/2}$ (min)
8	17.3	2.8
11	27.7	4.4
21	11.4	9
22	15.6	7.2
24	>60	6.5
26	44.3	15.5
28	81.7	19.4
29	58.9	63.8

Five selected benzoxazinone derived carboxamides (**8**, **11**, **21**, **22**, and **24**) were then subjected to in vitro metabolic stability tests in human and rat liver microsomes (HLM, RLM) (Table 3). All compounds demonstrated moderate to excellent stability in human microsomes but were markedly less stable in rat microsomes. It was also observed that fluorination on the nonpolar phenyl tail improved rat and human liver microsomal stability (**26**, **28**, and **29**). In fact, **29** not only possessed the best human and rat liver microsomal stabilities, but was also the most potent compound containing a 4*H*-benzo[1,4]oxazin-3-one polar head (Table 2).

We next turned our attention to additional modifications of the 4*H*-benzo[1,4]oxazin-3-one-containing polar head in order to increase functional potency. First, the 5-, 7-, and 8-position regioisomers (**30**–**32**) were prepared. None of these were superior to **29**. In fact, only the 7-isomer **31** showed any appreciable potency. The importance of a free oxazine NH (**29**) was confirmed by the complete eradication of activity by N-methylation (**33**). Replacement of the oxazine ring oxygen with sulfur also reduced functional activity by 33-fold (Table 4).

Numerous other modifications were made to the 4*H*-benzo[1,4]oxazin-3-one polar head, namely the addition of additional polar functionality at the 2-position. The majority of these were inactive, although esters **35** and **39** demonstrated relatively weak functional potency. Compound **41**, however, demonstrated remarkable potency (IC_{50} = 5 nM).

Compound **41** was stable in RLM ($t_{1/2}$ = 79 min) and in HLM ($t_{1/2}$ = 55 min), comparable with the parent molecule **29**. In addition, **41** was not a potent inhibitor of recombinant CYP enzymes (rCYP3A4 IC_{50} = 3.7 μM and rCYP2D6 IC_{50} > 10 μM). However, there was a potential for PGP-mediated efflux, as **41** demonstrated apical to basolateral transfer (A → B) across a Caco-2 cell monolayer with a $P_{app} = 1.5 \times 10^{-6}$ cm/s, but with a B → A/A → B ratio of 10.6.

Compound **41** was evaluated for in vivo efficacy in a rodent model of thermal hyperalgesia.[12] In the rat at an oral dose of 30 mg/kg, **41** produced a small but non-significant decrease in radiant heat latency at 30 min post-dose, as compared to 0.5% hydroxymethylcellulose vehicle (Fig. 3).

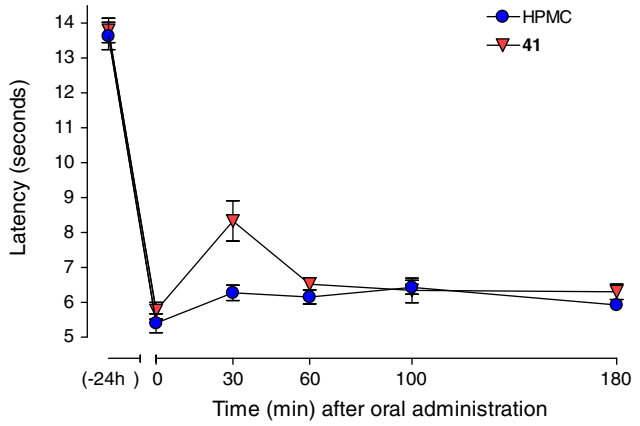

Figure 3. CFA radiant heat latency time course of **41**.

Table 4
Human TRPV1 functional potencies of optimized polar head substituents

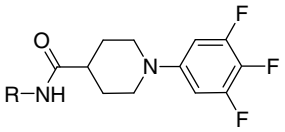

	R	Functional Potency % inh. or IC50 (μM)
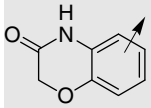	**30** 5-yl	9% inh. at 1 μM
	31 7-yl	55% inh. at 1 μM
	32 8-yl	Inactive
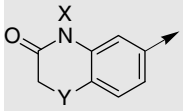	**33** X = Me, Y = O	Inactive
	34 X = H, Y = S	1.96 μM
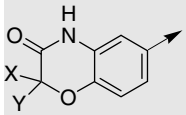	**35** X = Me, Y = CO_2Et	0.87 μM
	36 X = Me, Y = CO_2H	Inactive
	37 X = H, Y = CO_2Et	Inactive
	38 X = H, Y = CO_2H	Inactive
	39 X = H, Y = CH_2CO_2Me	0.89 μM
	40 X = H, Y = CH_2CO_2H	5% inh. at 1 μM
	41 X = H, Y = $(CH2)_2OH$	0.005 μM

In summary, a series of piperidine carboxamides were synthesized and tested, resulting in the identification of the lead candidate **41**. Due to potential dissolution-limited absorption and possible efflux, further optimization is underway to explore the potential of piperidine carboxamide TRPV1 antagonists for the treatment of pain.

References and notes

1. (a) Suh, Y.-G.; Oh, U. *Curr. Pharm. Design* **2005**, *11*, 2687; (b) Ferrer-Montiel, A.; Garcia-Martinez, C.; Morenilla-Palao, C.; Garcia-Sanz, N.; Fernandez-Carvajal, A.; Fernandez-Ballester, G.; Planells-Cases, R. *Eur. J. Biochem.* **2004**, *271*, 1820; (c) Owsianik, G.; D'hoedt, D.; Voets, T.; Nilius, B. *Rev. Physiol. Biochem. Pharmacol.* **2006**, *156*, 61; (d) Appendino, G.; Szallasi, A. *Prog. Med. Chem.* **2006**, *44*, 146.
2. Szallasi, A.; Cortwright, D. A.; Blum, Charles A.; Eid, S. R. *Nat. Rev. Drug Disc.* **2007**, *6*, 357.
3. (a) Valenzano, K. J.; Grant, E. R.; Wu, G.; Hachicha, M.; Schmid, L.; Tafesse, L.; Sun, Q.; Rotshteyn, Y.; Francis, J.; Limberis, J.; Malik, S. *J. Pharm. Exp. Ther.* **2003**, *306*, 377; (b) Swanson, D. M.; Dubin, A. E.; Shah, C.; Nasser, N.; Chang, L.; Dax, S. L.; Jetter, M.; Breitenbucher, J. G.; Liu, L.; Mazur, C.; Lord, B.; Gonzales, L.; Hoey, K.; Rizzolio, M.; Bogenstaetter, M.; Codd, E. E.; Lee, D. H.; Zhang, S.-P.; Chaplan, S. R.; Carruthers, N. I. *J. Med. Chem.* **2005**, *48*, 1857.
4. *Two general preparations of carboxylic acids: Method A.* Sodium *t*-butoxide (2.2 mmol) was added to a solution of phenyl halide Ar^1X (1.0 mmol), $Pd(OAc)_2$ (0.01 mmol), and 2-(di-*t*-butylphosphino)-biphenyl (0.02 mmol) in 5 ml of THF. After 5 min of stirring, isonipecotic acid (1.0 mmol) was added to the solution. The solution was heated to 65 °C for 18 h under an argon atmosphere, then cooled to rt and partitioned between EtOAc and water. The aqueous layer was separated and acidified using 3 N HCl and then extracted with EtOAc. The organic layer was washed with brine, dried over $MgSO_4$, filtered and concentrated to give the product.*Method B.* To a solution of ethyl isonipecotate (6.36 mmol) in 10 mL of anhydrous DME were added phenyl halide Ar^1X (9.54 mmol), bis(tri-*t*-butylphosphine)palladium(0) (0.636 mmol), and potassium phosphate (12.7 mmol). The reaction mixture was heated to 100 °C and stirred for 14 h. Solids were filtered off from the resulting mixture, and the collected filtrate was concentrated under reduced pressure to provide the crude product, which was then redissolved into 10 mL of methanol. Two milliliters of 1 N lithium hydroxide was added to hydrolyze the ester at 80 °C for 3 h. Solvent was evaporated, and the basic residue was acidified by 2 N HCl. The aqueous mixture was extracted with EtOAc. The combined organic layers were washed with brine, dried over $MgSO_4$, filtered, and concentrated under reduced pressure to afford the crude product, which was then purified by flash column chromatography with CH_2Cl_2 and CH_3OH to yield the product. *Two general preparations for amide coupling: Method C.* A solution of aniline Ar^2NH_2

(0.54 mmol) carboxylic acid (0.18 mmol), hydroxybenzotriazole (HOBt) (0.54 mmol) and triethylamine (0.54 mmol) in 1 mL *N*,*N*-dimethylformamide was treated with ethyl-3-(3 dimethylaminopropyl)-carbodiimide (EDC) (0.54 mmol). The solution was stirred at room temperature for 18 h. 5 mL of 10% K_2CO_3(aq) were added to the solution, which was then filtered. The solid was sequentially washed with water, CH_3OH and then dried in vacuo to afford the product. *Method D*. To a solution of carboxylic acid (0.122 mmol) in 5 mL of CH_2Cl_2 was added oxalyl chloride (0.244 mmol) and a catalytic amount of DMF. The reaction mixture was stirred for 2 h. Solvent was removed in vacuo. The residue was redissolved in 5 mL of CH_2Cl_2. Aniline Ar^2NH_2 (0.122 mmol) and triethylamine (0.183 mmol) were added sequentially into the acyl chloride solution at 0 °C. The reaction mixture was warmed to 25 °C and stirred for 20 min. Concentration of the solvent provided the residue, which was then purified by flash column chromatography with hexanes and ethyl acetate to afford the product. Spectral data have been reported: Calvo, Raul R.; Cheung, Wing S.; Player, Mark R. WO 06/058338.

5. The compounds were assayed for their ability to antagonize capsaicin-induced calcium flux using a Ca^{2+}-sensitive fluorescent dye and FLIPR™ technology (Molecular Devices Inc.). The [^{3}H]-RTX binding assay used hVR1/HEK293 cell membranes. Both assays were carried out under conditions previously reported. Jetter, M. C.; Youngman, M. A.; McNally, J. J.; Zhang, S. -P.; Dubin, A. E.; Nasser, N.; Dax, S. L. *Bioorg. Med. Chem. Lett.* **2004**, *14*, 3053–3056.
6. LigPrep, version 2.1, Schrödinger, LLC, New York, NY, 2005.
7. MacroModel, version 9.5, Schrödinger, LLC, New York, NY, 2007.
8. Phase, version 2.5, Schrödinger, LLC, New York, NY, 2007.
9. *c*log*P*, Daylight Chemical Information Systems, Inc., Aliso Viejo, CA, 2007.
10. QuickProp, version 3.0, Schrödinger, LLC, New York, NY, 2005.
11. JMP, version 6. SAS Institute Inc., Cary, NC, 1989–2005.
12. Complete Freunds adjuvant (CFA; 100 mL emulsion of saline and heat-killed *Mycobacterium tuberculosis* in mineral oil) was injected into a single hind paw of male Sprague–Dawley rats. Each rat was placed in a test chamber directly on a warm glass surface and acclimated for 10 min. Response latencies to the heat stimulus were recorded for each animal before and 24 h after the injection of CFA. Directly following the post-CFA latency measurement, test compound or hydroxymethylcellulose vehicle was administered orally to the animals. Post-treatment withdrawal latencies were assessed at 0, 30, 60, 100, and 180 min post-dose.